JOURNAL OF THE ROYAL SOCIETY Interface

J. R. Soc. Interface (2006) **3**, 441–451
doi:10.1098/rsif.2005.0097
Published online 14 December 2005

Characterization of the structure and composition of gecko adhesive setae

N. W. Rizzo, K. H. Gardner†, D. J. Walls, N. M. Keiper-Hrynko, T. S. Ganzke and D. L. Hallahan*

Central Research and Development, E.I. DuPont de Nemours and Company, Experimental Station, PO Box 80328, Wilmington, DE 19880-0328, USA

The ability of certain reptiles to adhere to vertical (and hang from horizontal) surfaces has been attributed to the presence of specialized adhesive setae on their feet. Structural and compositional studies of such adhesive setae will contribute significantly towards the design of biomimetic fibrillar adhesive materials. The results of electron microscopy analyses of the structure of such setae are presented, indicating their formation from aggregates of proteinaceous fibrils held together by a matrix and potentially surrounded by a limiting proteinaceous sheath. Microbeam X-ray diffraction analysis has shown conclusively that the only ordered protein constituent in these structures exhibits a diffraction pattern characteristic of β-keratin. Raman microscopy of individual setae, however, clearly shows the presence of additional protein constituents, some of which may be identified as α-keratins. Electrophoretic analysis of solubilized setal proteins supports these conclusions, indicating the presence of a group of low-molecular-weight β-keratins (14–20 kDa), together with α-keratins, and this interpretation is supported by immunological analyses.

Keywords: seta; adhesive; gecko; protein; keratin; β-keratin

1. INTRODUCTION

The adhesive setae of reptiles and insects have long fascinated biologists (Dellit 1934; Maderson 1964; Ruibal & Ernst 1965; Hiller & Blaschke 1967; Hiller 1968; Stork 1983), and interest in these structures has increased following recent demonstration of the adhesive properties of single, detached setae (Autumn *et al.* 2000). This work has led to speculation that synthetic mimics of these structures may be generated, yielding a new class of dry, reversible adhesive (Sitti & Fearing 2003). An understanding of the mechanism (Autumn *et al.* 2000, 2002) and mechanics (Jagota & Bennison 2002; Arzt *et al.* 2003; Persson 2003; Glassmaker *et al.* 2004; Hui *et al.* 2004) of adhesion of these structures is being developed. Proof of principle that artificial fibrillar arrays reminiscent of setae can, in fact, confer greater adhesive energy than unpatterned material has been published (Geim *et al.* 2003). However, the simple polymer fibrillar arrays fabricated thus far fall far short of the capabilities of the biological examples. We have undertaken a study of the structural and material properties of gecko setae in order to better understand the relationship between these properties and their role in reversible adhesion.

Reptilian setae, small bristles often mistakenly referred to as hairs, exist in two types. The most studied, typified by those present on the toe lamellae of the Tokay gecko *Gekko gecko* (figure 1), are multi-branched, hierarchical structures of 80–100 μm in length (Ruibal & Ernst 1965; Stork 1983; Schleich & Kastle 1986; Roll 1995). The second type, such as those found on the adhesive pads of anole lizards such as *Anolis carolinensis*, are smaller (*ca* 20 μm in length) and unbranched (Ruibal & Ernst 1965; Stork 1983). In all cases, arrays of many millions of such setae decorate the surface of the epidermal adhesive pads of these reptiles. The complex epidermis of these animals consists of a new (inner) generation, formed beneath the older (outer) generation, each generation consisting of six distinct layers. One of these layers, termed the β-layer, is known to accumulate β-keratins. The outer generation is shed during molting, and formation of a new inner generation initiated, such that during growth the animals replace the outer generation with a new generation at each shedding cycle. Individual reptilian setae are acellular, and previous studies (Maderson 1964; Ruibal & Ernst 1965) have indicated their origin as proteinaceous structures from the β-layer of the epidermal shedding complex of reptiles. These structures are in no case simple protein fibrils. In the geckos, setae are *ca* 100 μm in length, and their stalks, *ca* 3 μm in diameter at the base, branch repeatedly towards the distal end, generating an array of fibrils. Anolis setae

†Present address: Department of Materials Science and Engineering, University of Delaware, Newark, DE 19716-3106, USA.
*Author for correspondence (david.l.hallahan@usa.dupont.com).

The electronic supplementary material is available at http://dx.doi.org/10.1098/rsif.2005.0097 or via http://www.journals.royalsoc.ac.uk.

Received 31 August 2005
Accepted 14 November 2005

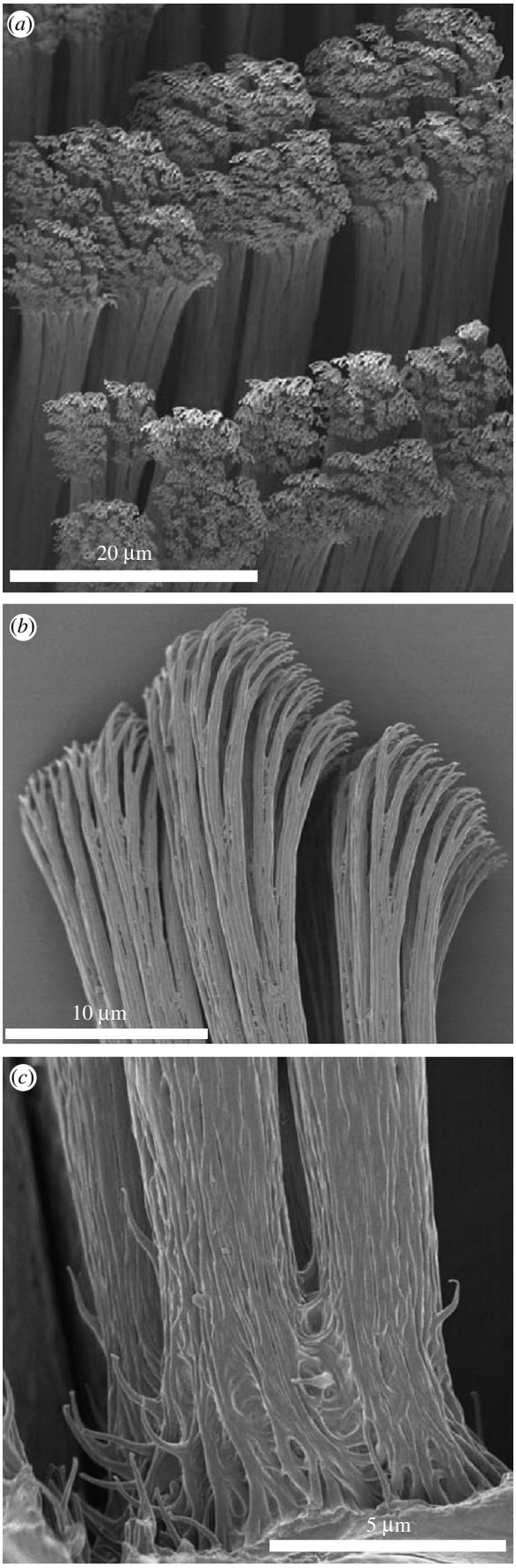

Figure 1. Scanning electron microscopy of *Gekko gecko* setae. (*a*) Setae attached to a section of toepad; and (*b*,*c*) detached setae. Separate full-size versions of the electron micrographs shown here can be found in the electronic supplementary material.

are shorter and do not subdivide, but even their stalks have a distinct conical shape. Both classes of setae bear specialized terminal elements at their distal ends, often termed 'spatulae' because of their resemblance to kitchen spatulae. These spatulae are triangular, and appear to flare out from the distal end of the setal stalk (in anoles) or terminal fibrils (in geckos).

That setae are composed of β-keratin protein was long assumed, and only recently has biochemical evidence emerged in support of this hypothesis (Alibardi 2003; Alibardi & Sawyer 2002). β-Keratins are present only in avian and reptilian epidermis, and an antiserum raised against an avian scale β-keratin was found to exhibit immuno cross-reactivity with gecko setae (Alibardi 2003). Strong immunofluorescent cross-reactivity was observed in mature setae of *Hemidactylus turcicus*, while labelling of the inner forming generation of setae was weaker. Using immunogold labelling, diffuse labelling was seen in mature setae, while in forming setae electron-pale inner filaments reacted with the antiserum, but the more electron-dense outer filaments did not.

Adhesive setae have arisen multiple times during the evolution of reptiles (Irschik *et al.* 1996). Although composed of different materials, many insect setae display remarkable similarity in structure to those borne by reptiles, including possession of spatular terminal elements (Stork 1983; Gorb 2001; Gorb & Beutel 2001). It is likely as a consequence that these terminal elements play a key role in adhesion of these structures.

How such structures assemble at the molecular level, the nature of their protein constituents, and how the properties of the proteins relate to those of the final structure is essentially unknown. In addition how, when formed, setae avoid clumping (despite their high aspect ratios), and how they (and their terminal elements) effect adhesion, remain to be solved, although these questions have been addressed in several recent publications (Jagota & Bennison 2002; Arzt *et al.* 2003; Persson 2003; Glassmaker *et al.* 2004; Hui *et al.* 2004). Recent work by Alibardi (1997) on the ontogeny of reptilian setae has shed considerable light on setal formation. Ultrastructural studies of setal formation in *A. lineatopus* have indicated that in this anole species, setae emerge from the oberhautchen layer of the epidermal shedding complex into the cells of the clear layer, which act as templates for their growth. It was also proposed that the clear layer cells template the formation of spatular terminal elements, and indeed apparently flattened setal termini were observed within the clear cell layer. This implies that, at least in anoles, setae are fully formed prior to shedding of the external epidermis during the shedding cycle. However, what mechanisms the cells of the clear layer employ to produce the setal (and spatulate) structure remain poorly understood (Alibardi 2003).

In this paper, we report progress on the characterization of the protein constituents of *G. gecko* setae. The data gathered will hopefully provide insight into the structure and properties of reptilian setae, leading to hypotheses on their development, particularly as regards the self-organization of constituent proteins

into the specialized terminal elements important for adhesion. An improved understanding of the nature of these structures should also assist in the design and development of synthetic mimics.

2. MATERIAL AND METHODS

2.1. Biological material

Animals (Tokay geckos, *G. gecko*) used in this study were obtained from Glades Herp, Inc. (Bushnell, FL, USA), and sacrificed immediately on receipt using CO_2 asphyxiation in accordance with DuPont corporate guidelines governing the care and use of animals in research. Detached setae were prepared by scraping along the toe lamellae with a fine dissecting needle after freezing individual toes in liquid nitrogen. The setae mostly broke-off at the base, yielding intact setae bearing the characteristic spatular structures at their fibrillated distal ends.

2.2. Scanning electron microscopy

Portions of Tokay gecko (*G. gecko*) toepads bearing setae were dissected and mounted on specimen supports. Detached setae, prepared as described above, were picked up onto carbon double-stick tape on a specimen mount by gently laying the sticky surface over the setae resting in a Petri dish, and lifting straight up, without applying any downward pressure. The specimens were sputter coated for 30 s with Au/Pd. The detached setae were imaged in a Hitachi 5000 SPX high-resolution Field Emission scanning electron microscopy (FESEM) and the toepads bearing setae were imaged in a Hitachi 4000 FESEM. Both instruments were operated at accelerating voltages between 1.0 and 2.5 kV.

2.3. Transmission electron microscopy

Portions of Tokay gecko (*G. gecko*) toepads bearing setae were dissected and fixed in 3% glutaraldehyde followed by post fixation in 2% osmium tetroxide. The toepads were dehydrated, infiltrated, embedded in Epon resin and cured at 60 °C. Ultrathin sections (*ca* 60 nm) were cut, picked up onto grids and the sections counterstained in 4% uranyl acetate followed by Reynold's lead citrate. Images were taken at an accelerating voltage of 200 kV on a Technai F-20 TEM.

2.4. X-ray diffraction

For collection of X-ray diffraction data, a piece of Tokay gecko toepad was mounted on a glass rod and positioned so that a diffraction pattern could be obtained from the group of setae (5-ID-B, $\lambda = 0.7$ Å, beam size 200 μm, Helium beam path, CCD detector (MarUSA, Inc.)). Microdiffraction experiments were performed on a similar piece of toepad. For the microdiffraction experiment, the X-ray beam was focused to a 2 μm spot size (50 mm focal length zone plate on the insertion device beamline), and diffraction patterns obtained every 4 μm on a 25×52 point grid (5-ID-D, $\lambda = 1.5$ Å, beam size 2 μm, helium beam path, CCD detector (MarUSA, Inc.)).

2.5. Raman spectroscopy

Raman spectra were obtained with a Renishaw Model 2000 Raman imaging microscope. Near infrared radiation at 785 nm generated from a Ti : sapphire laser system (Coherent) was used for excitation to minimize sample fluorescence. A 100× objective was used to focus the laser radiation to a 1 μm spot on the setae samples. A power level of 2 mW was used in all regions except very near the spatula region of the setae, where it was necessary to reduce to power level to 1 mW or lower to avoid sample damage. Detached individual setae were supported on Al coated microscope slides for Raman microscopy, using the integral optical microscope to position the sample for analysis.

2.6. Electrophoresis and Western analysis

Proteins were extracted from detached setae in a buffer containing 8 M urea, 3 mM ethylenediamine tetraacetic acid (EDTA), 125 mM β-mercaptoethanol, 200 mM Tris–Cl, pH 9.0. Following incubation overnight at 37 °C with gentle agitation, setae were removed by centrifugal filtration (Millipore Amicon Centricon). Two further sequential extractions of the undissolved setae thus collected were then carried out, in the same buffer including sodium dodecyl sulphate (SDS), first at 37 °C, and then at 100 °C. After filtration, each of the resulting protein solutions were analysed by electrophoresis. Denatured protein electrophoresis was conducted on 4–12% acrylamide gradient gels using a MES (4-morpholinethanesulfonic acid) buffer system (Invitrogen). Gels were stained with coomassie blue or proteins electroblotted to polyvinylidene fluoride (PVDF) membranes (Invitrogen) for Western blot analysis. Primary antisera used were a commercially available monoclonal anti-epithelial α-keratin (ICN 69-145-1; AE1/AE3 mix) and various anti-β-keratin antisera (Sawyer, R.H., University of South Carolina, USA). These were anti-β_1 (raised to chick scale β-keratin), universal β (raised to a β-keratin peptide fragment) and D_4 (raised to a feather-specific polypeptide from turkey vulture). All antisera were used at 1/500 dilution.

3. RESULTS AND DISCUSSION

3.1. Electron microscopy

In order to visualize more clearly the setae and their terminal elements, portions of Tokay gecko (*G. gecko*) toepads bearing setae and individual excised setae were examined using SEM (figure 1). SEM images of a dissected toepad revealed the length of Tokay gecko setae varied from *ca* 50 to 100 μm, with the shorter setae positioned at the front of each grouping on the toepad, as previously observed (Ruibal & Ernst 1965; Stork 1983; Schleich & Kastle 1986; Roll 1995). Also observed, as previously reported (Maderson 1964), was the remarkably ordered arrangement of setae on this

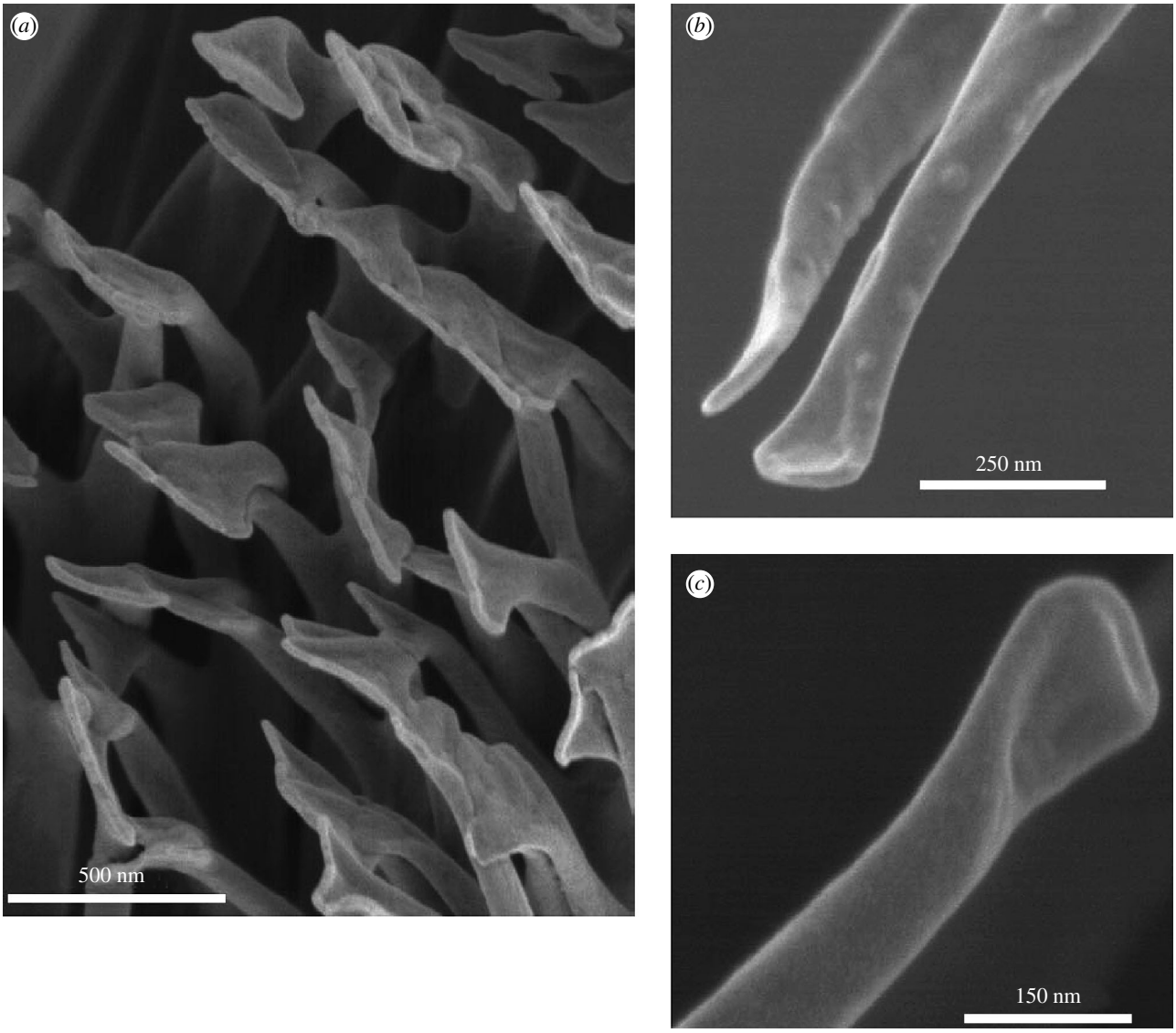

Figure 2. Scanning electron microscopy of the spatulate terminal elements of *Gekko gecko* setae. Detached setae were imaged to show (*a*) an array of spatule at the tip of a seta; and (*b*,*c*) details of individual spatulae. Separate full-size versions of the electron micrographs shown here can be found in the electronic supplementary material.

structure (figure 1*a*), although our observations indicated that setae emerged in groups of four. Closer examination of the distal and proximal portions of setae are shown in figure 1. At the distal end, each seta branches to produce bundles of fibrils, of some 130 nm in diameter at the point of branching, narrowing to *ca* 85 nm immediately prior to flaring out into spatulae. At the proximal end, setae emerge from a mat of fibrils of *ca* 100 nm in diameter, as observed by Stork (1983).

Detached setae were used for studies of the structure of the terminal spatulae (figure 2). Examination of SEM images showed that these triangular structures appeared to be formed by bifurcation of fibrils along *ca* 150 nm of their ends, with retention of a membrane of material between each branch (figure 2). The fibrils were *ca* 85 nm in diameter prior to branching, with each branch *ca* 50 nm towards its base but narrowing towards the end. At their furthest extremities, the spatulae were 150–275 nm across. The bifurcated/webbed structure, which could be observed in terminal spatulae, was also occasionally observed on the small fibrils towards the base of a seta. One of these, with its spatular end folded over, is shown in figure 2*c*. Similarly, prematurely truncated, spatula-bearing, filaments were observed by Ruibal & Ernst (1965) in setae of *Aristelliger praesignis*, although Stork (1983) observed in *G. gecko* such fibrils only tapering to points.

3.2. TEM

TEM was performed to examine the internal structure of setae as well as the structure of the spatula-shaped terminal elements. Ruibal & Ernst (1965) reported that the keratin that composes the setae of geckos and anoles is homogenous and showed no evidence of internal structure. Likewise, Roll (1995) observed from sections that developing setae of *Sphaerodactylus cinereus* were composed of many filaments, while mature setae showed no internal structure. TEM images of cross-sections of a mature *G. gecko* seta are shown in figure 3. From a cross-section of a seta prior to terminal branching (figure 3*a*), it can be seen that the seta is

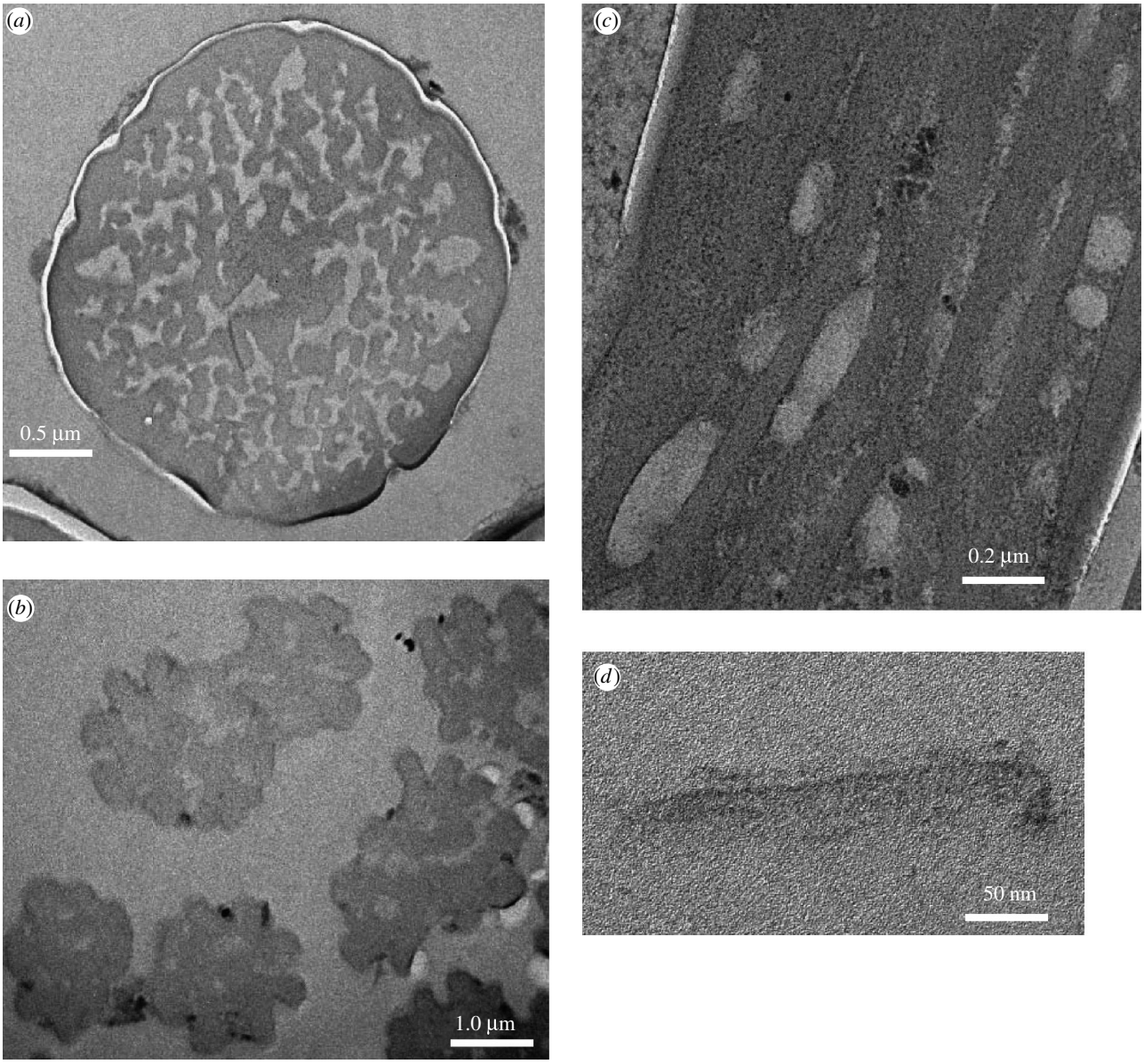

Figure 3. Transmission electron microscopy of sections through *Gekko gecko* setae. Sections of an individual detached seta at a point (*a*) before and (*b*) after initiation of terminal branching are shown, together with (*c*) a tangential section through a setal stalk; and (*d*) a single terminal spatula. Separate full-size versions of the electron micrographs shown here can be found in the electronic supplementary material.

clearly composed of individual fibrils within a less-densely stained matrix, surrounded by a sheath (see also Stork 1983). TEM of a mature seta at a point beyond the initiation of terminal branching (figure 3*b*) shows that the basic structure is the same although it would appear that the sheath is no longer present. Figure 3*c* shows a TEM image of a tangential section through a gecko seta, again showing the presence of individual fibrils and a matrix material bounded by a sheath. Where individual fibrils could be discerned in images such as this one, measurements of the fibril diameter yielded an average of 83 nm, very similar to the diameter of the terminal fibrils prior to flaring into spatulae. A section through the spatula-shaped terminal elements is shown in figure 3*d*. The thin central portion of the tip is *ca* 10 nm thick, and it is thought that this triangular, thin and presumably flexible 'membrane', supported on two-sides by the bifurcated end of a setal fibril, is responsible for the gecko's ability to conform to a surface and achieve effective adhesion. It would appear from these and the other studies cited that the individual fibrils seen in the setal shaft each terminate in one spatula tip at the end of each seta. An extensive TEM study involving serial sectioning would have to be undertaken to prove this hypothesis.

3.3. X-ray diffraction analysis

α-Keratins comprise a diverse group of molecules that have been extensively characterized by X-ray diffraction techniques as well as biochemical studies (Parry & Steinert 1999), while β-keratins have, by comparison, been much less studied. Patterns identified by X-ray diffraction analysis include the α-keratin pattern of mammals (also found in soft epidermal stratum

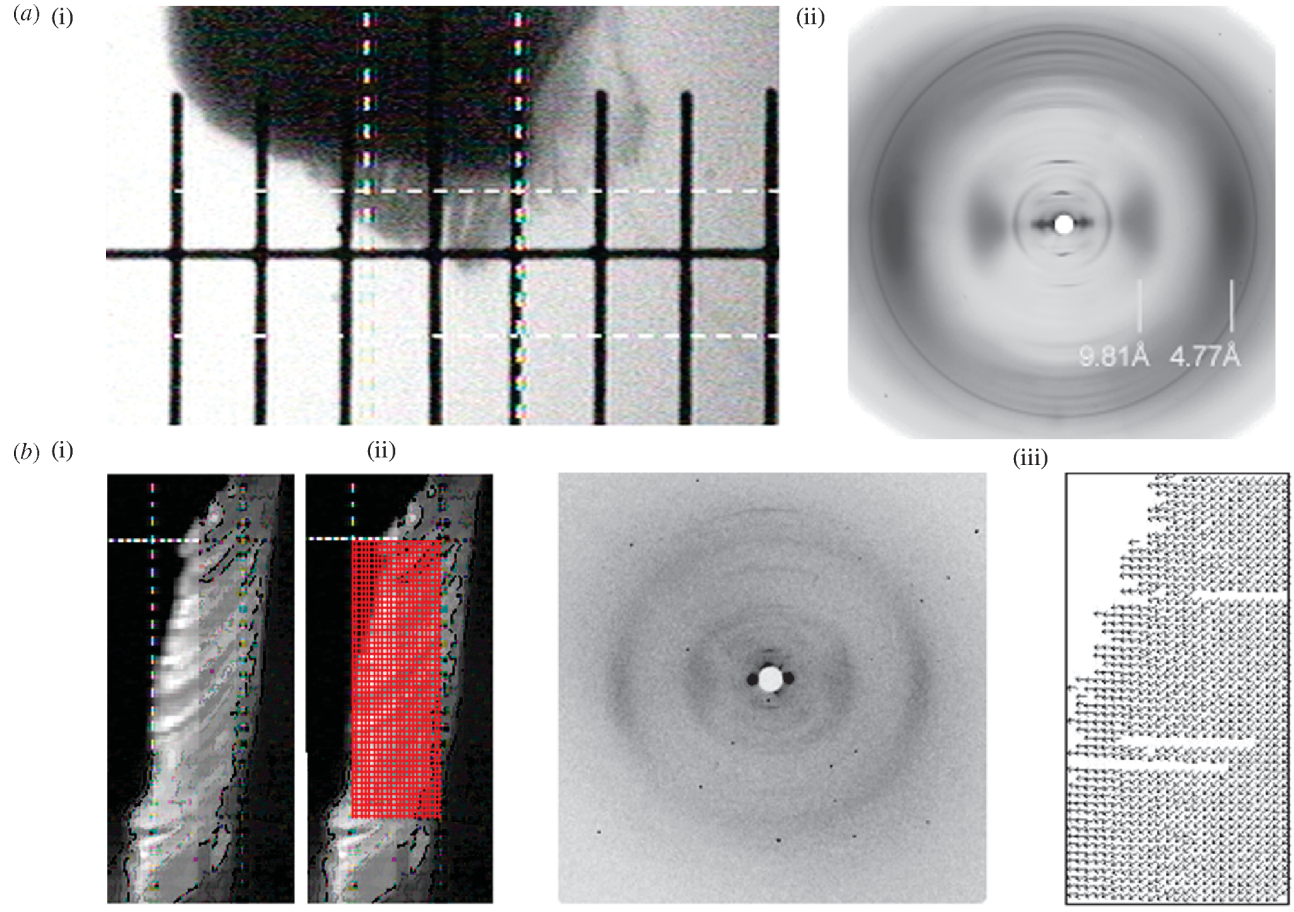

Figure 4. X-ray diffraction analysis of *Gekko gecko* setae. (*a*) A piece of Tokay gecko toepad was mounted on a glass rod (i), and the fibre diffraction pattern (ii) obtained from the group of setae contained in a 200 μm box (dashed white lines) is shown. (*b*) A beam focused to 2 μm was used to obtain the fibre diffraction pattern (ii) of a gecko toepad at each point within a grid of 4 μm by 4 μm squares (i). (iii) The angle of the principle axis of each of the diffraction patterns collected, plotted within the corresponding square of the grid.

corneum of reptiles and birds), and the β-keratin pattern of avian feathers and reptilian shells, beaks, claws and scales (Fraser *et al.* 1969, 1971; Fraser & Parry 1996). The unique structure of α-keratin is a modified α-helix (α-helical coiled coil) while that of β-type keratin is a twisted β-sheet. X-ray diffraction analysis shows that α-keratins exhibit a characteristic meridional diffraction spot at 5.1 Å and equatorial scattering at 9.8 Å. Reptilian β-keratin structures exhibit diffraction patterns with a strong equatorial low angle pattern, multiple meridional reflections and strong equatorial scattering at 9.5 and 4.7 Å (Fraser *et al.* 1972). We undertook diffraction studies to characterize further any ordered phase(s) present in setae and its secondary structure and orientation.

A piece of Tokay gecko toepad was mounted on a glass rod and the fibre diffraction pattern obtained from the group of setae contained in a 200 μm box is shown in figure 4. The pattern demonstrates all of the characteristics of a β-keratin diffraction pattern, with strong equatorial scattering at 9.81 and 4.77 Å, confirming that the setal material has the same structure as other previously studied reptilian epidermal material.

Microdiffraction experiments were also performed, on a similar piece of toepad. In the microdiffraction experiment the X-ray beam was focused to a 2 μm spot size and diffraction patterns obtained every 4 μm on a 26×52 point array. The microbeam diffraction patterns observed were characteristic of β-keratin in both the stalk and the spatular region of the setae, and an α-keratin diffraction pattern was not observed in any of these experiments. These diffraction patterns contain only four reflections, three equatorial and one meridional (figure 6). This paucity of reflections is likely due, at least in part, to the small sample mass in the beam. Fraser *et al.* (1972) reported that the avian keratin unit cell could be indexed on an orthorhombic unit cell with dimensions with dimensions $a=9.46$ Å, $b=9.7$ Å and c (fibre axis)$=6.68$. The 020 reflection (4.77 Å) corresponds to the interchain spacing between chains in the hydrogen bonded sheet. The 100 reflection (9.81 Å), which is larger than that reported by Fraser *et al.* (1972), corresponds to a repeat in the sheet packing direction. We have no explanation for this difference. Both the 23 Å meridional reflections and the 40 Å equatorial reflections could represent orders of low angle reflections that are hidden behind the beam stop. Analysis of the equatorial data of the diffraction patterns thus collected indicated that the molecular axes of the β-keratin ordered phase lie parallel to the local setal length axis. When taken with the results from SEM and TEM, this observation indicates that the β-keratin structural

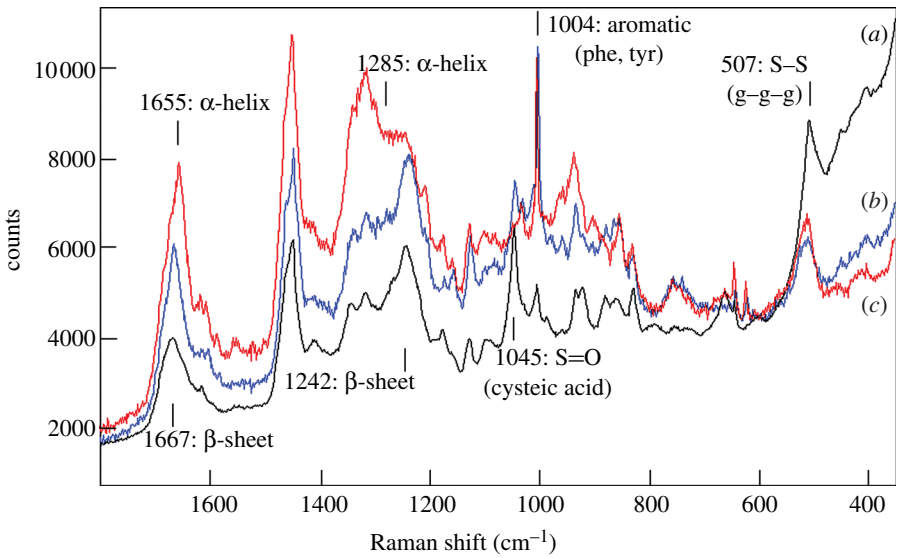

Figure 5. Raman spectroscopy of an individual *Gekko gecko* setal stalk. Raman spectra of the proximal stalk region of a single, detached, Tokay gecko seta (*a*), compared with that of avian feather (*b*) and merino sheep wool (*c*).

component essentially follows the same pattern as the fibrils observed using microscopy.

3.4. Raman microscopy

The Raman spectra of complex proteinaceous materials can yield considerable information on amino acid composition and secondary structure. Figure 5 shows three Raman spectra, obtained from white rock dove feather (primarily β-keratin; figure 5*a*), merino wool (α-keratin; figure 5*b*) and that obtained from the proximal end of a single *G. gecko* seta (figure 5*c*). It can be seen that the spectrum of the latter most resembles that from the avian feather, which is consistent with the known trends for avian and reptilian keratins (Edwards *et al.* 1993; Akhtar & Edwards 1997; Rintoul *et al.* 2000). The response observed from the amides I and III bands (near 1650 and 1250 cm^{-1}, respectively) associated with the polypeptide chains confirmed the predominance of β-keratin in the feather sample, and α-keratin in wool. The amide I band mainly involves the carbonyl stretching vibrations of the peptide backbone and is a sensitive marker of peptide secondary structure, since the vibrational frequency of each carbonyl bond depends on hydrogen bonding and the interactions between the amide units, both of which are influenced by the secondary structure (Twardowski & Anzenbacher 1994). The peak frequency change from 1655 to 1666 cm^{-1} in this band, going from the spectrum of wool to that of feather, is consistent with the change of predominant secondary structure from α-helix to beta sheet. Note that in both spectra, no one type of secondary structure accurately describes the entire sample and the observed carbonyl bands are typically a composite formed from the superposition of bands associated with the different types of secondary structure present in the sample. The amide III band, which involves a mixed vibration that involves CN and NH modes, is also fairly strong in the Raman spectra of proteins and its position also varies with changes in

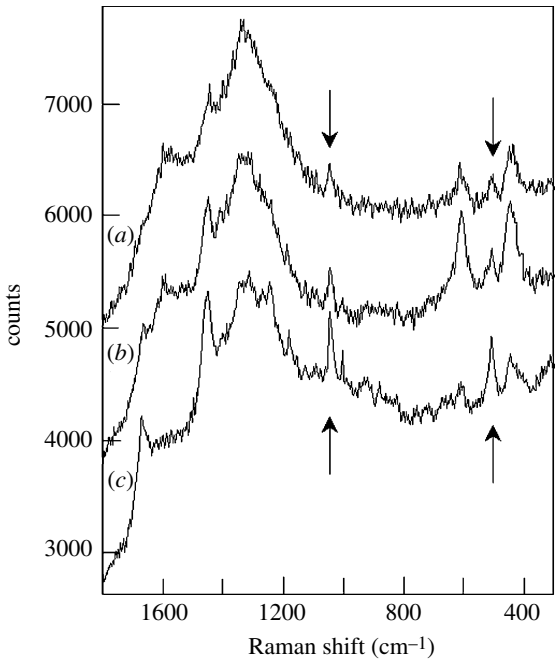

Figure 6. Raman spectroscopy of the distal end of an individual *Gekko gecko* seta. Raman spectra were collected from the distal spatular region of a single detached Tokay gecko seta (*a*), and at 10 μm (*b*) and 20 μm (*c*) proximal to this point. Indicated by arrows are bands associated with cysteic acid (1045 cm^{-1}) and disulphide cross-links (507 cm^{-1}).

secondary structure (Twardowski & Anzenbacher 1994). The spectra in figure 5 clearly show the predominance of β-sheet secondary structure in the feather sample, and infer the increased relative importance of structure associated with α-helical content in the wool sample. In the setal spectrum, both the amides I and III regions show the predominant signature of β-keratin, although the underlying band shape suggests that there is a significant level of α-keratin and/or protein with a random coil structure.

While not considered a primary tool for the characterization of primary structure, some amino

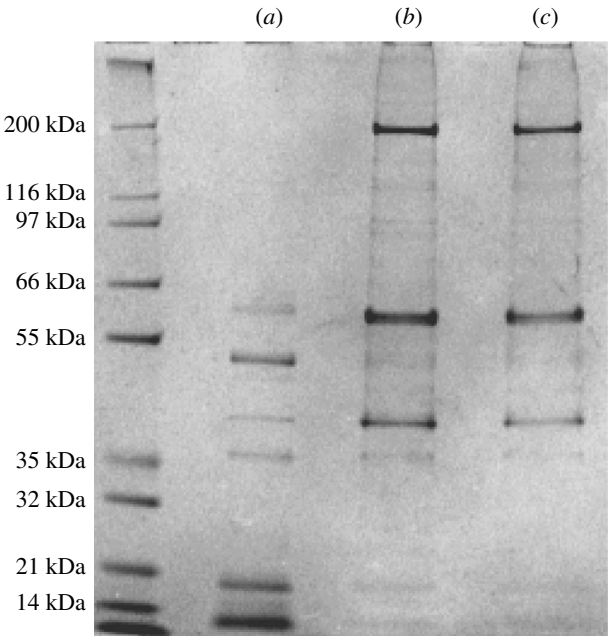

Figure 7. Gel electrophoretic analysis of *Gekko gecko* setal proteins. Solubilized setal proteins were separated on 4–12% acrylamide gels and stained with Coomassie Blue. (*a*) proteins extracted with urea and β-mercaptoethanol; (*b*) proteins extracted with urea, β-mercaptoethanol and SDS (37 °C); (*c*) proteins extracted with urea, β-mercaptoethanol and SDS (100 °C).

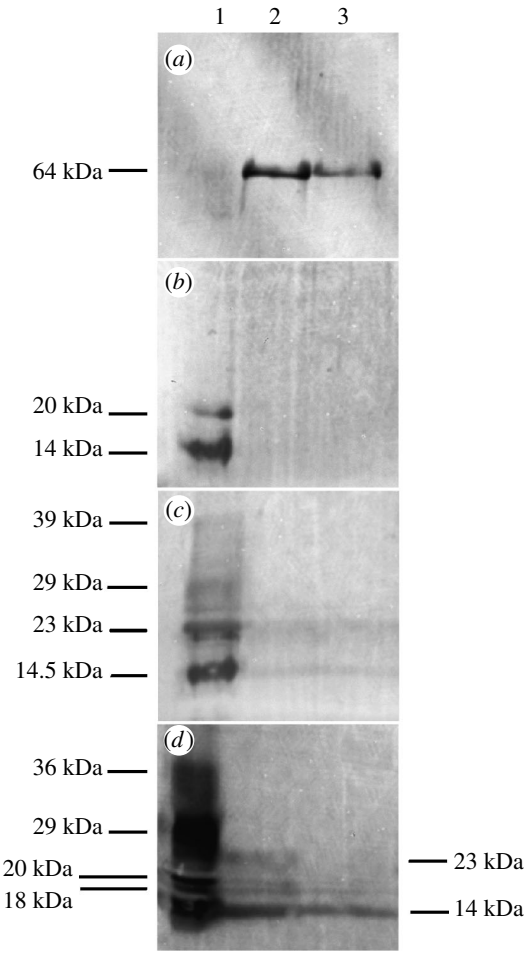

Figure 8. Western analysis of *G. gecko* setal proteins. Solubilized gecko setal proteins were separated by electrophoresis, and immunoreactivity with anti-keratin antisera probed after transfer to PVDF membranes. (*a*) AE1/AE3 anti-α-keratin monoclonal antibodies, (*b*) antiserum D_4 (to feather β-keratin), (*c*) anti-β_1 antiserum (to chick scale β-keratin); (*d*) universal anti-β-keratin (to β-keratin peptide). Lane 1, proteins extracted with urea and β-mercaptoethanol. Lane 2, proteins extracted with urea, β-mercaptoethanol and SDS (37 °C). Lane 3, proteins extracted with urea, β-mercaptoethanol and SDS (100 °C).

acids provide characteristic bands that permit their identification and structural analysis with Raman spectroscopy. Sulphur containing residues are one class, where Raman spectroscopy proves quite powerful and is recognized as being one of the best methods for examining conformational structure in disulphide bridges which occur in proteins. The band near 507 cm^{-1} indicates the presence of disulfide cross-linkages and is present in all of the samples studied (figure 5). This location is consistent with a g–g–g conformation between the C–S–S–C linkages in the disulfide linkages (Akhtar & Edwards 1997; Akhtar *et al.* 1997; Edwards *et al.* 1998). However, unlike the other samples, the setal spectrum shows very little intensity as well as a different pattern of intensities for bands associated with sulphide groups, suggesting that the cysteine residues present near the proximal end of the gecko setae are highly cross-linked. This, along with the predominance of β-keratin in this region of the structure, suggests that the material in this portion of the gecko setae may be quite stiff. A significant difference observed in the spectrum of the gecko seta relative to the other spectra in figure 5 was the presence of a much stronger band near 1045 cm^{-1}, which we assign to the S=O groups associated with cysteic acid (Akhtar *et al.* 1997). The presence of these oxidized groups could go along with the relative lack of evidence for free cysteine residues in this spectrum.

The aromatic amino acid residues—phenylalanine, tyrosine, tryptophan, and histidine—have strong and unique Raman bands that can be used to establish their presence and relative abundance in a particular protein. In figure 5*a*,*b*, a strong aromatic band is observed near 1004 cm^{-1} that is likely associated with phenylalanine or tyrosine residues. This band is apparently of weaker intensity in the setal spectrum (figure 5*c*). A doublet with peaks at 830 and 850 cm^{-1} and a pair of bands near 1173 and 1206 cm^{-1} are consistent with the presence of tyrosine in all samples. The presence of a strong band at 507 cm^{-1}, with little contribution from bands centred near 525 and 540 cm^{-1}, indicates the predominant presence of disulfide linkages with gauche conformational linkages along the C–S–S–C linkages in all samples. Bands near 622, 642, 740 and 755 cm^{-1}, weak in the setal spectrum, are all associated with sulphide residues from cysteine and methionine residues.

A series of measurements were also made as a function of position along the length of a typical *G. gecko* seta, at 10 μm intervals over a length of 80 μm, starting at the proximal end. The Raman spectra thus obtained (not shown) varied very little with position. From this analysis, it would appear that the primary and secondary structure did not change

significantly with position over this length-scale near the proximal end of the seta.

It proved more difficult to obtain Raman spectra near the spatula end of the setae, due to changes in the structure of the setae with laser exposure. Using the same conditions used to obtain spectra from the proximal end (2 mW focused into a 1 μm spot), we found that the setae would immediately move out of focus, indicating they were presumably very sensitive to localized heating associated with laser exposure. This is opposed to the proximal end of the setae that do not show significant changes in either position or spectral response even with higher power levels. This observation in and of itself suggests a structural difference exists between these regions of the seta. With lower power levels, we did obtain Raman spectra towards the distal end of setae, which revealed differences that potentially explain this response. Figure 6 shows Raman spectra obtained from the last 20 μm of the setae in 10 μm intervals using 1 mW of power focused into a 1 μm spot. It is this region which is most susceptible to laser-induced heating effects. The spectra obtained (figure 6) did change considerably within this region, perhaps most significantly in those bands associated with sulphur-containing groups. The band at 507 cm^{-1}, associated with disulfide cross-linkages, decreased in intensity as the spatula tip region was approached. This suggests that the material within the spatula tip region is less cross-linked and perhaps softer than the material in the proximal end of the setae. This would also explain the increased thermal liability observed within this region. The response associated with cysteic acid also decreased as the tip of the setae was approached, suggesting perhaps that there are fewer sulphur-containing groups near the spatula tips relative to the content near the proximal end.

3.5. Denaturing gel electrophoresis of extracted setal proteins

In order to analyse protein composition by gel electrophoresis, setae were collected-off the toe lamellae of a Tokay gecko by first freezing the toes in liquid nitrogen, then scraped-off setae using a dissecting needle. Routinely, setae were then suspended in a buffer containing 8 M urea, 3 mM EDTA, 125 mM β-mercaptoethanol, 200 mM Tris–Cl, pH 9.0, and incubated at 37 °C with gentle agitation overnight. Microscopic examination at the end of this incubation indicated that setae from different animals dissolved to different extents by this treatment. We, therefore, subjected the setae to two further sequential extractions, in the presence of SDS at 37 °C and then at 100 °C. After filtration, the resulting protein solutions were analysed by denaturing gel electrophoresis (LDS-PAGE). This analysis showed that in samples from all animals sacrificed, one or more members of three major classes of proteins could be observed. Bands of high (*ca* 120 kDa) and medium (77, 64 and 54 kDa) apparent molecular weight could be distinguished, together with at least one band of lower apparent molecular weight (*ca* 18 kDa). However, in certain animals some of these bands were not effectively extracted. We hypothesized that these differences might be a consequence of the stage of the animal within its shedding cycle, and thus sacrificed an animal that was known to have shed within the past 2 days. The results of LDS-PAGE of setal protein extracts from this animal are shown in figure 7. In this gel, most of the bands noted above are present, together with an additional high molecular weight band (200 kDa). The initial extraction, in the absence of SDS, yielded principal bands with apparent molecular weights of 14, 19 and 53 kDa, and minor bands of 36, 42 and 64 kDa. Extraction in the presence of SDS yielded bands of 200, 62 and 41 kDa, and fainter bands of 139, 121, 114, 52, 47 and 36 kDa could be discerned. It can also be seen that the setal constituent proteins are differentially extracted, with the lower molecular mass proteins extracted in the absence of detergent, whereas added detergent was required to extract the higher molecular mass proteins.

In order to identify potential α- and β-keratins in these extracts, the immuno cross-reactivity of these proteins to antisera specific to these protein classes was analysed by Western blotting of setal proteins separated on by electrophoresis (figure 8). One of the proteins present in gecko setae, of 64 kDa, cross-reacted with anti-α-keratin antiserum (figure 8*a*). This antiserum also lightly labelled lower molecular mass bands likely to be β-keratins (not shown), thus was not entirely specific towards α-keratins in this reptilian material. As regards the low molecular weight species, their cross-reactivities were consistent with their assignment as β-keratins. All three β-keratin antisera tested, one of which was previously shown to cross-react with setae (Alibardi 2003), labelled the polypeptides of between 14 and 20 kDa present in setal protein extracts. The antiserum raised to avian feather β-keratin labelled only these two proteins (figure 8B), while the universal β and anti-β_1 (Sawyer *et al.* 2000) antisera labelled several additional bands (figure 8*c*,*d*), notably those with molecular masses of 39, 29, 23, 20, 18 and 14 kDa. The anti-β_1 antiserum also faintly labelled bands of higher molecular mass (62 and 54 kDa), as did the universal β (62 kDa), thus these antisera may not be entirely specific for β-keratins.

In comparing the proteins separated by electrophoresis (figure 7) with those labelled by Western blot analysis (figure 8), it is apparent that several proteins which could be extracted from setae did not exhibit cross-reactivity with the antisera available. The identity of these setal constituents (200, 53 and 42 kDa proteins) thus remains ambiguous.

4. CONCLUSIONS

Characterization of gecko setae using electron microscopy has shown that these structures consist of bundles of fibrils, which branch out distally and terminate in characteristic 'spatular' terminal elements. Our observations support the contention that the fibrillar structure is preserved over the length of the seta, with fibrils observed to yield spatulae at the distal end of setae likely to traverse the entire length of the seta. In some cases, fibrils which terminate prematurely towards the base of a seta also possess spatulate terminal elements. It would seem unlikely,

due to the complexity of gecko setae, that fibril expansion into spatulae be 'templated' or 'moulded' in some way by the tissues of the shedding complex. Our observation of spatulae on prematurely terminated fibrils might imply that in fact the propensity to form spatulae is inherent in the fibrils themselves. Prior to this study, little was known about the protein constituents of reptilian setae other than they likely included β-keratin. Thus to expand on such observations, we undertook a study of the protein constituents of setae. Our goal was to provide structural information about the proteins present in the setae, and to see if any structural changes occurred from the proximal end (base or attachment point) of the setae to the spatular feature at the distal end. Features that could differentiate mechanical properties of the structure through differences in protein structure or any features that could help better understand the adhesion process from a structure/property standpoint were sought. X-ray diffraction studies of setal arrays showed that the only ordered regions in Tokay gecko setae had a β-keratin structure in which the axes of the chains are aligned parallel to the axis of the setae. Microdiffraction allowed us to follow the structure through a setal array from the base of the stalks through to the spatulate region at the tips. The same β-keratin pattern was observed in both the stalk and spatular region. No evidence of an ordered α-keratin phase was observed. It would be surprising if such complex structures were generated from a single class of proteins, thus we took advantage of the high spatial resolution and sensitivity to protein secondary structure that Raman microscopy provides to examine *G. gecko* setae for other protein constituents. Raman spectroscopy is useful for studying proteins due to its ability to distinguish and characterize protein secondary structure. It is also not limited in application to ordered or crystalline structures as is the technique of X-ray diffraction. The amides I and III absorbtion bands associated with polypeptide chains (whose exact position in the spectrum depends on the dihedral angles ψ and φ that change with secondary structure) are readily observed with this technique. This provides an effective means to differentiate α-helical, beta sheet, and random coil secondary structural forms. Our analysis revealed that β-sheet secondary structure predominated within the setal shaft, although spectral features associated with α-helical content were also observed. Additionally, this analysis indicated a high degree of disulfide cross-linking of the setal protein constituents. Disulfide linkages associated with g–g–g conformational states were readily observed, although bands associated with free methionine or cysteine groups were relatively absent. Studies of structure as a function of position near the proximal end of the setae showed little change in either secondary or primary structure over an 80 μm interval starting at the base of the setae. Studies of structure as a function of position near the setal tips suggested decreased cross-linking associated with the presence of a softer, more deformable, material in this region. This might suggest the presence of a very different type of structure in this region, but more likely is consistent simply with the thinness of the spatulae.

The results of gel electrophoretic analysis of extracted setal proteins were also consistent with the setae being composed of both α- and β-keratins. Although, both α- and β-keratins have been identified in reptilian epidermal tissues, it had been presumed that setae were either entirely or predominantly composed of β-keratins. However, LDS-PAGE indicated the presence of proteins with apparent molecular weights greater than would be expected for β-keratins in setal extracts, at least one of which cross-reacted with anti-α-keratin antibody. Given the masses and immuno cross-reactivities of the proteins observed in such extracts, it would appear likely that they comprise both α- and β-keratins. How these proteins are assembled into such a complex structure as a gecko seta, and especially how the sub-filaments within these structures differentiate at their tips into spatulate terminal elements, remains to be fully elucidated. The work described here on the compositional analysis of setae we hope will provide new insight into, and stimulate future studies of, these fascinating structures.

The authors are grateful to R. Sawyer, University of South Carolina, for provision of the anti-β-keratin antisera, and J. D. Londono and R. V. Davidson, DuPont, for their assistance with the microdiffraction experiments. The X-ray diffraction experiments were performed at the DuPont-Northwestern-Dow Collaborative Access Team (DND-CAT) Synchrotron Research Center located at Sector 5 of the Advanced Photon Source. DND-CAT is supported by the E. I. DuPont de Nemours & Co., The Dow Chemical Company, the US National Science Foundation through grant DMR-9304725 and the State of Illinois through the Department of Commerce and the Board of Higher Education grant IBHE HECA NWU 96. Use of the Advanced Photon Source was supported by the US Department of Energy, Office of Science, Office of Basic Energy Sciences, under Contract No. W-31-109-Eng-38.

REFERENCES

Akhtar, W. & Edwards, H. G. M. 1997 Fourier-transform Raman spectroscopy of mammalian and avian keratotic biopolymers. *Spectrochim. Acta, A: Mol. Biomol. Spectrosc.* **53A**, 81–90.

Akhtar, W., Edwards, H. G. M., Farwell, D. W. & Nutbrown, M. 1997 Fourier-transform Raman spectroscopic study of human hair. *Spectrochim. Acta, A: Mol. Biomol. Spectrosc.* **53A**, 1021–1031. (doi:10.1016/S1386-1425(97)00055-3)

Alibardi, L. 1997 Ultrastructural and autoradiographic analysis of setae development in the embryonic pad lamellae of the lizard Anolis lineatopus. *Ann. Sci. Nat. Zool. Biol. Anim.* **18**, 51–61.

Alibardi, L. 2003 Ultrastructural autoradiographic and immunocytochemical analysis of setae formation and keratinization in the digital pads of the gecko *Hemidactylus turcicus* (Gekkonidae, Reptilia). *Tissue Cell* **35**, 288–296. (doi:10.1016/S0040-8166(03)00050-8)

Alibardi, L. & Sawyer, R. H. 2002 Immunocytochemical analysis of beta (beta) keratins in the epidermis of chelonians, lepidosaurians, and archosaurians. *J. Exp. Zool.* **293**, 27–38. (doi:10.1002/jez.10145)

Arzt, E., Gorb, S. & Spolenak, R. 2003 From micro to nano contacts in biological attachment devices. *Proc. Natl Acad. Sci. USA* **100**, 10 603–10 606. (doi:10.1073/pnas.1534701100)

Autumn, K., Liang, Y. A., Hsieh, S. T., Zesch, W., Chan, W. P., Kenny, T. W. & Fearing, R. 2000 Adhesive force of a single gecko foot-hair. *Nature* **405**, 681–685. (doi:10.1038/35015073)

Autumn, K., Sitti, M., Liang Yiching, A., Peattie Anne, M. & Hansen, M. 2002 Evidence for van der Waals adhesion in gecko setae. *Proc. Natl Acad. Sci. USA* **99**, 12 252–12 256. (doi:10.1073/pnas.192252799)

Dellit, W.-D. 1934 Zur anatomie und physiologie der geckozehe. *Jena J. Naturw.* **68**, 613–656.

Edwards, H. G. M., Farwell, D. W., Williams, A. C. & Barry, B. W. 1993 Raman spectroscopic studies of the skins of the Sahara sand viper, the carpet python and the American black rat snake. *Spectrochim. Acta, A: Mol. Biomol. Spectrosc.* **49A**, 913–919. (doi:10.1016/0584-8539(93)80210-2)

Edwards, H. G. M., Hunt, D. E. & Sibley, M. G. 1998 FT-Raman spectroscopic study of keratotic materials: horn, hoof and tortoiseshell. *Spectrochim. Acta, A: Mol. Biomol. Spectrosc.* **54**, 745–757. (doi:10.1016/S1386-1425(98)00013-4)

Fraser, R. D. B. & Parry, D. A. D. 1996 The molecular structure of reptilian keratin. *Int. J. Biol. Macromol.* **19**, 207–211. (doi:10.1016/0141-8130(96)01129-4)

Fraser, R. D. B., MacRae, T. P., Parry, D. A. D. & Suzuki, E. 1969 Structure of beta-keratin. *Polymer* **10**, 810–826. (doi:10.1016/0032-3861(69)90110-4)

Fraser, R. D. B., MacRae, T. P., Parry, D. A. D. & Suzuki, E. 1971 Structure of feather keratin. *Polymer* **12**, 35–56. (doi:10.1016/0032-3861(71)90011-5)

Fraser, R. D. B., MacRae, T. P. & Rogers, G. E. 1972 *Keratins: their composition, structure and biosynthesis.* Springfield, Ill.: Thomas.

Geim, A. K., Dubonos, S. V., Grigorieva, I. V., Novoselov, K. S. & Zhukov, A. A. 2003 Microfabricated adhesive mimicking gecko foot-hair. *Nat. Mater.* **2**, 461–463. (doi:10.1038/nmat917)

Glassmaker, N. J., Jagota, A., Hui, C.-Y. & Kim, J. 2004 Design of biomimetic fibrillar interfaces: 1. Making contact. *J. R. Soc. Interface* **1**, 23–33. (doi:10.1098.rsif.2004.0004)

Gorb, S. N. 2001 Attachment devices of insect cuticle. New York: Springer.

Gorb, S. N. & Beutel, R. G. 2001 Evolution of locomotory attachment pads of hexapods. *Naturwissenschaften* **88**, 530–534. (doi:10.1007/s00114-001-0274-y)

Hiller, U. 1968 Studies on fine structure and function of the digital setae of reptiles. *Z. Morphol. Tiere* **62**, 307–362. (doi:10.1007/BF00401561)

Hiller, U. & Blaschke, R. 1967 [On the fastening problem of gecko feet] Zum Haftproblem der Gecko-Fusse. *Naturwissenschaften* **54**, 344–345. (doi:10.1007/BF00621466)

Hui, C.-Y., Glassmaker, N. J., Tang, T. & Jagota, A. 2004 Design of biomimetic fibrillar interfaces: 2. Mechanics of enhanced adhesion. *J. R. Soc. Interface* **1**, 35–48. (doi:10.1098/rsif.2004.0005)

Irschik, D. J., Austin, C. C., Petren, K., Fisher, R. J., Losos, J. B. & Ellers, O. 1996 A comparative analysis of clinging ability among pad-bearing lizards. *Biol. J. Linn. Soc.* **59**, 21–35. (doi:10.1006/bijl.1996.0052)

Jagota, A. & Bennison, S. J. 2002 Mechanics of adhesion through a fibrillar microstructure. *Integr. Comp. Biol.* **42**, 1140–1145.

Maderson, P. F. A. 1964 Keratinized epidermal derivatives as an aid to climbing in gekkonid lizards. *Nature* **203**, 780–781.

Parry, D. A. D. & Steinert, P. M. 1999 Intermediate filaments: molecular architecture, assembly, dynamics and polymorphism. *Q. Rev. Biophys.* **32**, 99–187. (doi:10.1017/S0033583500003516)

Persson, B. N. J. 2003 On the mechanism of adhesion in biological systems. *J. Chem. Phys.* **118**, 7614–7621. (doi:10.1063/1.1562192)

Rintoul, L., Carter, E. A., Stewart, S. D. & Fredericks, P. M. 2000 Keratin orientation in wool and feathers by polarized Raman. *Biopolymers* **57**, 19–28. (doi:10.1002/(SICI)1097-0282(2000)57:1<19::AID-BIP4>3.0.CO;2-Z)

Roll, B. 1995 Epidermal fine structure of the toe tips of *Sphaerodactylus cinereus*. *J. Zool.* **235**, 289–300.

Ruibal, R. & Ernst, V. 1965 The structure of the digital setae of lizards. *J. Morphol.* **117**, 271–293. (doi:10.1002/jmor.1051170302)

Sawyer, R. H., Glenn, T., French, J. O., Mays, B., Shames, R. B., Barnes, G. L., Rhodes, W. & Ishikawa, Y. 2000 The expression of beta keratins in the epidermal appendages of reptiles and birds. *Am. Zool.* **40**, 530–539.

Schleich, H. H. & Kastle, W. 1986 Ultrastrukturen an Gecko-Zehen. *Amphibia-Reptilia* **7**, 141–166.

Sitti, M. & Fearing, R. S. 2003 Synthetic gecko foot-hair micro/nano-structures as dry adhesives. *J. Adhes. Sci. Technol.* **17**, 1055–1073. (doi:10.1163/156856103322113788)

Stork, N. E. 1983 A comparison of the adhesive setae on the feet of lizards and arthropods. *J. Nat. Hist.* **17**, 829–836.

Twardowski, J. & Anzenbacher, P. 1994 *Raman and IR spectroscopy in biology and biochemistry*, pp. 107–121. Chichester, UK: Ellis Horwood.